

# New Geometry for the Enhancement of the Raceway Pond Performance

OUSSAMA GHANNEM<sup>1,2</sup>, HAYTHEM NASRAOUI<sup>2</sup>, ZIED DRISS<sup>2</sup>

<sup>1</sup>National School of Engineers of Tunis (ENIT),  
University of Elmanar,  
Tunis,  
TUNISIA

<sup>2</sup>Laboratory of Electro-Mechanic Systems (LASEM),  
National School of Engineers of Sfax (ENIS),  
University of Sfax,  
TUNISIA

**Abstract:** - This work aims to enhance the hydrodynamic properties of microalgae production units which can solve the issue of the energy demand and the environmental problem of the world. The studied system is a raceway pond built in Monastir city in Tunisia. By using the commercial CFD software, ANSYS Fluent, a set of simulations was created to assess the hydrodynamic characteristics of the pond. The results were verified through the experimental measurements of the fluid velocity in both channels of the system. The standard k- $\epsilon$  turbulence model was used to model the turbulence created by the paddle wheel of the fluid flow. Two design parameters were studied in this paper. The impact of the configuration of the bend system's endpoint on the behavior of the pond was investigated by altering two radii. The numerical findings align well with the experimental observations.

**Key-Words:** - Raceway ponds, CFD model, Energy, Microalgae production, radii Bend, Hydrodynamic, Experimental measurements, Design.

Received: June 11, 2024. Revised: September 16, 2024. Accepted: November 17, 2024. Published: December 31, 2024.

## 1 Introduction

In recent times, the interest in the algae industry has led to the development of various applications for the food and bioenergy markets, [1]. In fact, the most fundamental and cost-effective cultivation system for microalgae production is open raceway ponds. While microalgae productivity in open raceway ponds is lower compared to other cultivation systems like photobioreactors, this is often offset by their relatively low capital and operating costs, as well as the high economic value of their products, [2]. In commercial operations, raceways are the most successful technologies for cultivating the large-scale production of algae, [3]. Open algae cultivation systems come in a wide range of configurations in terms of size, construction materials, agitation systems, and overall design, [4]. A RWP is made up of a shallow pond divided into two or more channels, according to the proposed general design. The liquid stream is agitated by a mechanical rotor, which generates a turbulent flow inside the pond. The RWPs are the

most commonly used open culture systems, owing to their relatively low construction costs, ease of maintenance, low energy requirements, and scalability, [5]. For high productivity and energy efficiency, it's critical and difficult to achieve a uniform distribution of nutrients, CO<sub>2</sub>, light, mixing, and algal cells in an ORP. In open raceway pond systems, paddle wheels are commonly used as the mixing mechanism to generate the required water flow velocity and ensure effective circulation throughout the pond channels. A Uniform flow mixing by a paddle wheel is therefore required to bring algae cells from the pond's bottom to the top surface and expose them to sunlight. The turbulent mixing generated by the paddle wheel also enhances nutrient transfer from the water to the algae cells by causing some damage to their cell membranes, [6]. The yield of microalgae production initially increases with increasing turbulence, most likely due to an improved supply of CO<sub>2</sub> or a higher frequency of dark-light cycles. But, after reaching an optimum value, the yield rapidly degrades with increasing turbulence. However, this shear stress

characteristic has yet to be investigated in large-scale open pond systems. Furthermore, the impact of the pond's geometry on hydrodynamic characteristics has yet to be thoroughly fully investigated, potentially leading to an incomplete understanding of the design result. Power consumption is another important design parameter because it influences the economics and productivity of algae biomass, [7]. Hydraulic power was used to generate liquid velocity in the channel, which accounts for the majority of the power consumption. The actual power for a given raceway channel will be determined by the length of the raceway's channel. A longer pond requires more energy to move the water along the channel, and the shape of the bends will also affect the amount of energy required to circulate the water flow. As a result, the evaluation of pond design power is critical. Although light is necessary for algal growth, too little or too much light will limit or inhibit the photosynthetic process, [8]. The performance of mixing was determined by the design of RWP in terms of circulation velocity ( $V_c$ ), shear stress ( $\tau$ ), and the presence of a dead zone, [9]. In commercial RWP, a velocity of 0.15 m/s to 0.3 m/s is commonly required for algae cultivation, [10]. Algae cells are sensitive to hydrodynamic forces, [11], [12], and the cell damage caused by shear stress has been one of the major challenges to overcome when developing artificial algae cultivation systems, [13]. In RWP, high velocities and a high degree of mixing can harm the algae cells' growth. The areas where mixing velocities are not sufficient (that's when  $> 0.1$  m/s) are known as dead zones or stagnant zones. Dead zones reduce the physical volume of the pond, as well as the time spent there, and have an impact on cultivation productivity, [14]. Numerous studies have been carried out to investigate the design of open raceway ponds to reduce energy consumption and improve the growing efficiency of microalgae, [15]. A significant portion of the energy is lost at the sharp turns or hairpin bends in the ponds. Various bend configurations using computational fluid dynamics (CFD), [16]. When compared to the traditional constant-width/constant-depth bend configuration, these authors demonstrated that some of the new bend configurations not only minimize energy consumption but also improve raceway pond mixing by overcoming low speed and stagnant regions, [16]. Another CFD-based approach demonstrated that, in addition to being more energy-efficient than the standard configuration, a raceway configuration with at least three semicircular

deflector baffles and an "island" at the end of the central divider can completely prevent the development of dead zones, [17]. The majority of recent design studies on open raceway ponds rely on modeling and simulations, with only a small number utilizing actual experiments. Regardless of how the models and associated technologies progress, there will always be discrepancies when comparing the model results to experimental data, [18], [19]. This study compared the performance of two raceway ponds with different configurations based on three criteria: areal productivity, energy consumption, and the biochemical composition of biomass produced using *Nanochloropsis oceanica* as a model microalga. Simple bend designs are not optimal for biomass growth because they result in large areas of stagnant flow and high energy loss. A raceway system measuring 630 m in length, 4 m in width, and 0.3 m in depth was analyzed using theoretical CFD, powered by a conventional 8-blade paddlewheel and operating at a fluid velocity of 0.14 m/s, [20]. The percentage of dead zones around the bends was found to be as high as 14.2% of the total area, according to the authors. Similar results were observed in a raceway measuring 5 m in width, 96 m in length, and 0.3 m in depth, operating at a fluid velocity of 0.3 m/s, which accounted for 18% of the total area, [21]. The fluid depth increases around the side walls of the bend. This increase in depth is referred to as superelevation, [22]. It is caused by the fluid's desire to continue in a straight line and the wall's exertion of a force to prevent it from doing so. This causes a pressure difference across the channel section, resulting in the formation of flows transverse to the main flow, [23]. Secondary flows are transverse flows that, when combined with the main forward flow, create a helicoidal flow, [24]. Other research has proposed that there is a constant total head across the width of the channel and as a consequence of the increased depth there must be a reduction in the velocity head, [25]. Research from the CFD showed that the 180° end bends provide the vertical speed to be mixed up five times more than that of the straight sections, [26]. Furthermore, other experimental work has shown that end bends increase the dispersion coefficient, which is a measure of fluid mixing, by two-fold [27]. Other bend designs that combined flow deflectors and island configurations have been investigated, [28]. This option was the best of the ones that were simulated because it had the lowest total power requirement, a reduction of 18% over the standard configuration, and no dead zones in the

raceway. However, when compared to the design with three deflectors, this design reduces power by only 1.5%, but it necessitates a much more complex construction, which may result in higher capital costs. From these interiors studies, it is clear that the study of the algae open ponds is very crucial and require more investment.

The present paper describes the hydrodynamic flow properties of algae open ponds and how they can be used to optimize algae pond designs. The hydrodynamic flow conditions are related to power consumption, dead zone occurrence, global shear stress characteristics, and variations in pond geometry and dimension, such as end bends by using the Computational Fluid Dynamics (CFD) modeling. This paper's approach emphasizes the need for more research into large-scale raceway design.

## 2 CFD Method

### 2.1 Mathematical Model

This part describes the basic physical models provided by the CFD code. The present problem can be solved in a steady-state simulation. In fact, three-dimensional steady simulations are performed by using the commercial CFD code ANSYS FLUENT 17.0. This code is based on Navier-Stokes equations to predict the fluid flow inside the raceway pond. To calculate fluid behavior in the raceway pond, the equations governing the flow are the fundamental three-dimensional fluid mechanic equations for mass, momentum, and energy conservation. They can be written in the cartesian coordinates as follows

$$\frac{\partial \rho}{\partial t} + \frac{\partial}{\partial x_i} (\rho u_i) = 0 \quad (1)$$

$$\frac{\partial}{\partial t} (\rho u_i) + \frac{\partial}{\partial x_j} (\rho u_i u_j) = -\frac{\partial p}{\partial x_i} + \frac{\partial}{\partial x_j} \left[ \mu \left( \frac{\partial u_i}{\partial x_j} + \frac{\partial u_j}{\partial x_i} - \frac{2}{3} \delta_{ij} \frac{\partial u_k}{\partial x_k} \right) \right] + \frac{\partial}{\partial x_j} (-\rho \overline{u_i' u_j'}) + F_i \quad (2)$$

The considered turbulence model is the standard k-ε model. The turbulence kinetic energy k, and its rate of dissipation, ε are obtained from the following transport equations:

$$\frac{\partial}{\partial t} (\rho k) + \frac{\partial}{\partial x_j} (\rho k u_j) = \frac{\partial}{\partial x_j} \left[ \left( \mu + \frac{\mu_t}{\sigma_k} \right) \frac{\partial k}{\partial x_j} \right] + G_k + G_b - \rho \varepsilon - Y_M + S_k \quad (3)$$

$$\frac{\partial}{\partial t} (\rho \varepsilon) + \frac{\partial}{\partial x_i} (\rho \varepsilon u_i) = \frac{\partial}{\partial x_j} \left[ \left( \mu + \frac{\mu_t}{\sigma_\varepsilon} \right) \frac{\partial \varepsilon}{\partial x_j} \right] + C_{1\varepsilon} \frac{\varepsilon}{k} (G_k + C_{3\varepsilon} G_b) - C_{2\varepsilon} \frac{\varepsilon^2}{k} + S_\varepsilon \quad (4)$$

The turbulent (or eddy) viscosity  $\mu_t$  is computed by combining k and ε as follows:

$$\mu_t = \rho C_\mu \frac{k^2}{\varepsilon} \quad (5)$$

Constants of the standard k-ε model are presented in Table 1.

Table 1. Constants of the standard k-ε model

$C_{1\varepsilon}$	$C_{2\varepsilon}$	$C_\mu$	$\sigma_k$	$\sigma_\varepsilon$
1.44	1.92	0.09	1.0	1.3

### 2.2 Reference System

To minimize the energy losses at the raceway bends, which can improve the efficiency of open raceway pond algae cultivation systems, it is important to reduce the resistance of the fluid flow resistance at those bend locations, numerical modeling for a shallow turbulent flow in a rectangular channel was performed by using the commercial CFD code ANSYS Fluent 17.0. A paddlewheel drives the microalgae suspensions cultured in the RWPs to flow constantly through the circuit. Figure 1 presents the raceway pond, the used paddle wheel, and the culture microalgae of this system. The length and width of the simulated RWP in this paper were set to 23.5 m and 3.8 m, respectively. A paddlewheel with three blades and a radius of 0.4 m was also installed at one of the RWP's straight channels.



Fig. 1: Experimental system

## 2.3 Geometrical and Meshing Domains

The coordinate system for a typical raceway bend is shown in Figure 2, where  $L$  is the length of the transition section,  $R$  is the channel width, and  $r$  is the radius of curvature. Besides, the width of the central divider is assumed to be 0.2m. Furthermore,  $d$  denotes the local depth, and  $d_0$  denotes the standard channel depth, the thickness of the central divider wall between two straight channels was set to 0.5 m.  $R = 5\text{m}$  and  $d_0 = 0.3\text{m}$  were chosen for this study. The RWP design requires an accurate choice of end bend geometry by changing the radius of curvature  $R_1$  (table 3) and  $R_2$  (table 2). This process must allow for favorable hydrodynamic conditions, such as good mixing, the elimination of dead zones and short-circuits, and low shear stresses. Thus, the aim is to obtain minimal consuming power.

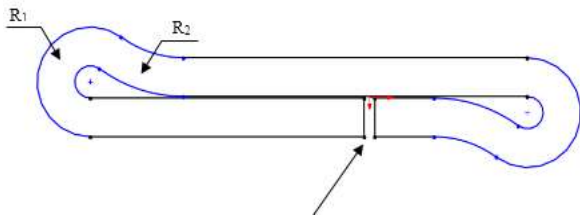


Fig. 2: Raceway bend geometry as shown for a standard raceway pond

Table 2. Variation of the head radius

$R_1$	2	2.5	3	3.5
$R_2$	1	1	1	1

Table 3. Variation of the medium radius

$R_2$	2	2.5	3	3.5
$R_1$	1	1	1	1

In this study, we, first, changed the head radius curvature in end bends and we fixed the medium radius. In the next phase, we take the inverse course and we study their hydrodynamic effects. An unstructured tetrahedral mesh was used for all simulations in which the radius of curvature was varied. For the meshing, an unstructured hexahedral mesh (Figure 3) with an aspect ratio that allowed for finer spacing in the vertical direction rather than in the horizontal direction, which was used for all computations in which the channel's end bends are constant. Tetrahedral meshes are typically made up of 1,000,000 elements, while hexahedral meshes are made up of 300,000 elements. It should be noted that the RWP system's 3-dimensional geometry is

created in ANSYS Design Modeler 17.0 and meshed by structured mesh in ANSYS Meshing 17.0. In the meshed RWP system, we have obtained 353648 cells.



Fig. 3: Meshing of the computational domain.

## 2.4 Theoretical Approach

The pressure difference between given points after and before the paddle wheel is used to describe the power, which represents the paddle wheel's energy consumption. The pressure was calculated and then the power was formulated:

$$P = Q \Delta p \quad (6)$$

where  $Q$  is the fluid flow and  $\Delta p$  is the pressure difference created by the paddle wheel.

A dead zone is created when a large eddy flow occurs, resulting in a stagnant flow at the middle wall's end. Because calculating the dead volume is difficult, we propose using the following assumption. We used this value as the threshold for the existence of dead zones and then quantified the dead volume because the lowest fluid velocity required to avoid settling of algae cells in the pond is 0.1 m/s, [27].

$$\% D_v = \frac{V_{v<0.1}}{V_{\text{pond}}} \times 100\% \quad (7)$$

where  $V_{(v<0.1)}$  is the volume of liquid with a velocity less than 0.1 m/s and  $V_{\text{pond}}$  is volume of liquid in the pond.

The location of low velocity (we call the dead zone) can easily cause stacking and death of algae during microalgae cultivation. The proportion of the dead area should be reduced to avoid this microalgae cultivation phenomenon.

## 3 Results and Discussion

### 3.1 Power

Figure 4 and Figure 5 show the changes in the consumed power by the rotor when varying the radii  $R_1$  and  $R_2$ . It can be seen from these results that the power consumption decreases with the increase in the bend radius  $R_1$ . The power consumption in this case, reaches approximately 74% of the standard bend design. The power is reduced when changing

the medium radius 4.8% from the standard design. However, focusing solely on power consumption ignores other, less obvious financial savings. These are possible savings in capital costs, electrical engineering, and other economies of scale because the ponds, such as end bends, can take more superficialities. As an example of the latter effect, authors claim that increasing the area of a raceway pond facility by a factor of ten ,reduces the cost of algae per kg (dry weight) by a rate of 75%.

This may be an overly optimistic estimate. But, if the scaling is roughly linear, increasing the size of the raceway ponds by a factor of two implies a potential reduction in the algae's "per kg" cost of the order of 5%. Of course, constructing a more complex pond design will almost certainly increase the construction cost. We are hoping to get quantitative estimates for this additional cost from businesses that want to build ponds using the designs in this paper.

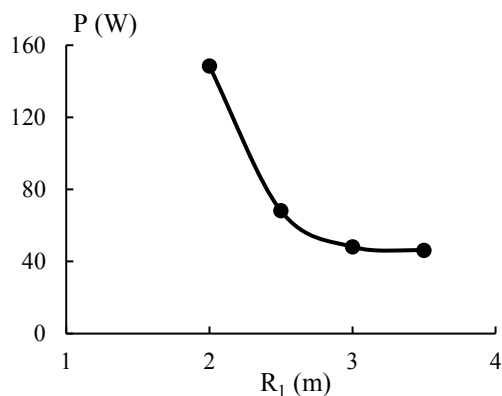


Fig. 4: Channel hydraulic power consumption for the various head radius bend geometries 4.8

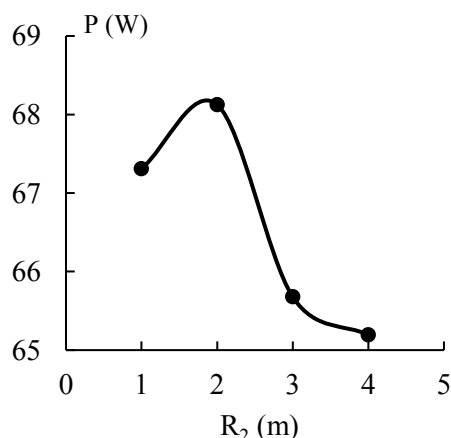


Fig. 5: Channel hydraulic power consumption for the various medium radius

### 3.2 Dead Zone

To study the effect of the presence of a paddle wheel on the formation of dead zones, the fraction of dead zone volume is calculated using equation (7). A large dead zone volume is generally expected in small-sized and medium-sized ponds because of the non-uniform pond velocity produced by the paddle wheel. However, the fraction of dead zone volume can be reduced by increasing the value of the head radius (Figure 6). This reduction is at its maximum for  $R_1 = 4$  m. By increasing  $R_1$  the presence of large eddies decreases in favor of small eddies. A higher head radius in the channel will thus increase the dispersion of the cells and the dead zone volume subsequently dispersed as shown in different dispersions of dead zones in Figure 8 (Appendix). However, the correlation between  $R_1$  and volume eddies is linear.

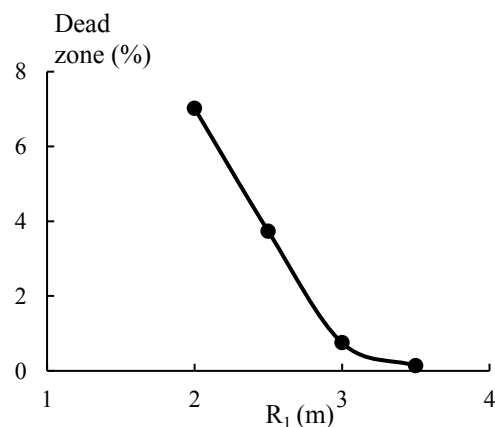


Fig. 6: Dead zone in the various  $R_1$  size of ponds

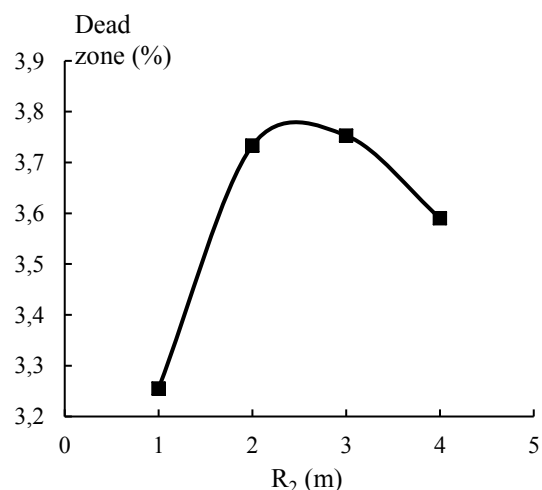


Fig. 7: Dead zone in the various  $R_2$  sizes of ponds

To minimize the effect of dead zones on algae cell production, pond geometry must be optimized in accordance with paddle wheel rotational speed. Moreover, at a constant rotational speed of 13 rpm, an increase in  $R_2$  increases slightly in a very negligible way (Figure 9, Appendix). Consequently, a more prominent rising of medium radius in end bends is depicted along with an augmented volume of dead zones at the end of the center wall for all cases as shown in Figure 7. The flow is not directly circulated  $180^\circ$  by this modification, resulting in a more uniform velocity field in the channel compared to the previous pond design, since the improvement of the hydraulic properties.

### 3.3 Static Pressure

Figure 10 and Figure 11 in Appendix show the distribution of the static pressure in all proposed geometries. According to these results, it has been observed that the high-pressure zones appear after the paddle wheel and the low-pressure zones appear before it. This obvious change in the static pressure is due to the location of the momentum source which simulated the force provided by the variation in  $R_1$ . The decrease in the static pressure with different  $R_1$  along the straights illustrates the effects of raising the head radius for better pressure distribution. However, from the results in Figure 10 (Appendix), it is obvious that the static pressure has a similar distribution as the standard one. The advancing and the returning channels have different pressure distributions. Indeed, higher pressure values are noted on the indirect side of the pond and lower values are noted on the direct side. The maximum values  $p=319$  Pa are obtained when we rise  $R_2 = 3.5$  m. Thus, the increase in the medium radius increases slightly the pressure difference.

### 3.4 Magnitude Velocity

Figure 12 and Figure 13 in Appendix show the distribution of the velocity magnitude in all geometries. According to these results, it has been observed that in the standard case the acceleration zones appear at the end bend when the fluid changes its direction. Then, the water velocity decreases gradually to reach the minimum value at the system center. However, a uniform distribution of the velocity magnitude appears when changing the radii of the bent end. The best distribution is shown with  $R_1 = 3.5$  m. Figure 12 (Appendix) shows that the increase of bend radius  $R_2$  has no effect on the behavior of water velocity. Enhanced performance is indicated by the absence of localized acceleration

which creates a dead zone. Therefore, the raceway bond with  $R_1 = 3.5$  m presents a good solution to decrease the dead zone and increase the performance of the system.

### 3.5 Turbulent Kinetic Energy

Figure 14 and Figure 15 in Appendix depict the distribution of the turbulent kinetic energy in all proposed geometries. From these results, it can be seen that the high turbulent kinetic energy is shown in the standard case. However, it has been observed that the turbulent kinetic energy presents the same distribution for other cases. This means that the proposed design of a pond with a circular bend presents an efficient solution to reduce the turbulent kinetic energy. The increase of the first radius  $R_1$  decreases the turbulent kinetic energy. Meanwhile, the change of the second radius  $R_2$  does not have a large effect on the turbulent kinetic energy distribution. In fact, in the cases of  $R_2=2$  m and  $R_2=4$  m, it presents the low values. In these cases, the maximum value is reached near the bend region. Otherwise, this turbulent region is great at the entrance of the paddle wheel zone, when the paddle wheel is located far from the bend zone. However, the peak value of the turbulent kinetic energy decreases in the other shapes. In these cases, it can be seen that the fluid turbulence appears along both channels. This fact leads to enhancing of the performance of microalgae production.

### 3.6 Comparison with Experimental Data

The potential of algal biomass production in an ORP with two culture radii of 0.4m (Figure 16) and 0.5m (Figure 17) has been estimated.



Fig. 16: Experimental system which  $R_1=0.4$ m

As is evident from Figure 18 the new design with a change of radius from 0.4 m to 0.5 m



improves the productivity of algae. These results confirm the validity of our numerical method.



Fig. 17: Experimental system which  $R_1=0.5m$

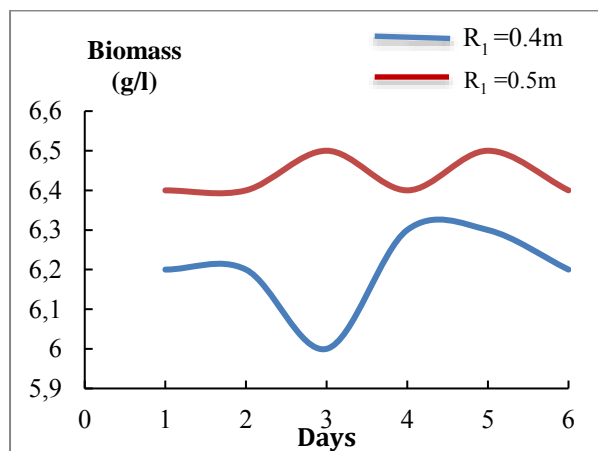


Fig. 18: Evolution of biomass with different radius

### 3.7 Mass Transfer

The geometry of the raceway pond plays a critical role in determining flow patterns, which directly influences the efficiency of microalgae cultivation. Optimizing the shape by adjusting the head and medium radii can enhance turbulence, which is essential for improving mass transfer rates. Increased turbulence facilitates better mixing of microalgae with nutrients and gases, promoting more effective absorption of  $CO_2$  from the atmosphere. The implementation of internal structures, referred to as R2, can disrupt laminar flow and induce turbulence, thereby enhancing contact between the liquid and gas phases crucial for effective mass transfer.

Furthermore, increasing  $R_1$  to create a wider pond can provide a greater surface area for  $CO_2$  absorption. However, it is important to balance this width with the need for adequate mixing to prevent

stagnation. The optimal design should achieve a balance between maximizing light capture and enhancing mass transfer, ensuring that microalgae remain in optimal growth conditions, as illustrated in Figure 18.

## 4 Conclusions

In this paper, a series of simulations were developed in order to validate the hydrodynamic characteristics of the pond. The results were validated by the experimental measurements of the fluid velocity in both channels of the system. The standard k- $\epsilon$  turbulence model was used to model the turbulence created by the paddle wheel of the fluid flow. The effect of the shape of the end of the bending system on the pond behavior was examined by changing two radii. These results will be used for the enhancements of the raceway pond design.

To mitigate energy consumption, minimize dead zones, and reduce the intensity of shear stress in raceway ponds, we conducted a thorough evaluation of various bend geometries with different radii. This assessment aimed to identify optimal designs that enhance fluid dynamics within the ponds. By systematically analyzing how different geometrical configurations impact flow characteristics, we sought to improve the overall efficiency and performance of the raceway systems. The findings from this study will contribute significantly to the design strategies for raceway ponds, ultimately leading to more sustainable algae cultivation practices.

Several of the newly designed bends, particularly the "head radius" and "medium radius box" configurations, not only reduce energy consumption but also enhance mixing within the raceway pond. By effectively eliminating low-speed and stagnant regions in the flow, these designs have the potential to significantly boost algae productivity in raceway systems.

On the whole, this progressed vitality effectiveness of the modern raceway pond designs will allow the plan of bigger ponds with lesser relative investment to conceivably minimize the ultimate generation cost of algae growth.

Future work could focus on the development and testing of more complex geometric configurations beyond the head and medium radius adjustments. Exploring non-linear shapes and innovative internal structures may lead to even greater improvements in flow dynamics and mass transfer rates.

### Acknowledgements:

Authors may acknowledge to any person, Laboratory of Electro-Mechanic Systems (LASEM) that supported any part of the study.

### Declaration of Generative AI and AI-assisted Technologies in the Writing Process

During the preparation of this work the authors used Grammarly for language editing. After using this service, the authors reviewed and edited the content as needed and take full responsibility for the content of the publication.

### References:

- [1] Rasal, V. M., Yadre, S. G., Shukla, S. P., Ravi, P., Mishra, M. K., Munilkumar, S., Pal, A. K., Lakra, W., & Dasgupta, S. (2019). Microalgae distribution and diversity in the Narmada river basin around Chutka, Madhya Pradesh, India. *International Journal of Current Microbiology and Applied Sciences*, 8, 1488–1501. <https://doi.org/10.20546/ijcmas.2019.809.171>.
- [2] Tredici, M., Chini Zittelli, G., & Rodolfi, L. (2009). Photobioreactors. In *Wiley Encyclopedia of Industrial Biotechnology*, Vol. 4, pp. 1-14. John Wiley & Sons. <https://doi.org/10.1002/9780470054581.eib479>.
- [3] Crowe, B., Attalah, S., Agrawal, S., & Waller, P. (2012). A comparison of Nannochloropsis salina growth performance in two outdoor pond designs: Conventional raceways versus the ARID pond with superior temperature management. In *Proceedings of the 2012 Algal Biomass Summit* (pp. 1-8). Denver, CO. <https://doi.org/10.1155/2012/920608>.
- [4] Weissman, J. C., & Goebel, R. P. (1987). Design and analysis of pond systems for the purpose of producing fuels. *Final Report, Solar Energy Research Institute*, Golden, CO, SERI/STR, 231-2840. <https://doi.org/10.2172/6546458>.
- [5] Mendoza, J.L., Granados, M.R., de Godos, I., Ación, F.G., Molina, E., Banks, C. and Heaven, S. (2013). Fluid dynamic characterization of real-scale raceway reactors for microalgae production. *Journal of Biomass and Bioenergy*, 54, 267–275. <https://doi.org/10.1016/j.biombioe.2013.03.017>.
- [6] Chen, Z., Zhang, X., Jiang, Z., Chen, X., He, H., & Zhang, X. (2016). Light/dark cycle of microalgae cells in raceway ponds: Effects of paddlewheel rotational speeds and baffles installation. *Bioresource Technology*, 219, 387-391. <https://doi.org/10.1016/j.biortech.2016.07.108>
- [7] Dodd, J. C. (1986). *Elements of pond design and construction*. In A. Richmond (Ed.), *Handbook of Microalgal Mass Culture* (pp. 45-60). CRC Press.
- [8] Brune, D. E., Schwartz, G., Eversole, A. G., & Collier, J. A. (2003). Intensification of pond aquaculture and high rate photosynthetic systems. *Aquacultural Engineering*, 28, 65–86. [https://doi.org/10.1016/S0144-8609\(03\)00025-6](https://doi.org/10.1016/S0144-8609(03)00025-6).
- [9] Pruvost, J., Le Borgne, F., & Legrand, J. (2009). Modelling photobioreactors for mass scale solar production of microalgae. In *Proceedings of the 8th World Congress of Chemical Engineering* (p. 25), Montreal, Canada, 23-27 August 2009.
- [10] Chiaramonti, David, Prussi, Matteo, Casini, David, Tredici, Mario, Rodolfi, Liliana, Bassi, Niccolo, Chini Zittelli, Graziella, Bondioli, Paolo. (2013). Review of energy balance in raceway ponds for microalgae cultivation: Rethinking a traditional system is possible. *Applied Energy*, 102, 101–111. <https://doi.org/10.1016/j.apenergy.2012.07.040>.
- [11] Barbosa, M. J., Hadiyanto, & Wijffels, R. H. (2004). Overcoming shear stress of microalgae cultures in sparged photobioreactors. *Biotechnology and Bioengineering*, 85, 78–85. <https://doi.org/10.1002/bit.10862>.
- [12] Silva, H. J., Cortiñas, T., & Ertola, R. J. (1987). Effect of hydrodynamic stress on Dunaliella growth. *J. Chem. Technol. Biotechnol.*, 40, 41–49. <https://doi.org/10.1002/jctb.280400105>.
- [13] Jackson, B. A., Bahri, P. A., Moheimani, N. R. (2017). Repetitive non-destructive milking of hydrocarbons from Botryococcus braunii. *Renewable and Sustainable Energy Reviews*, 79, 1229–1240. <https://doi.org/10.1016/j.rser.2017.05.130>.
- [14] Qinghua Zhang, Shengzhang Xue, Chenghu Yan, Xia Wu, Shumei Wen, Wei Cong (2015). Installation of flow deflectors and wing baffles to reduce dead zone and enhance



- flashing light effect in an open raceway pond. *Bioresource Technology*, 198, 150–156. <https://doi.org/10.1016/j.biortech.2015.08.144>
- [15] Kusmayadi, A., & Suyono, E. A. (2020). Application of computational fluid dynamics (CFD) on the raceway design for the cultivation of microalga. *Journal of Industrial Microbiology and Biotechnology*, 47(4-5), 373–382. <https://doi.org/10.1007/s10295-020-02273-9>.
- [16] Cunha, P.; Pereira, H.; Costa, M.; Pereira, J.; Silva, J. T.; Fernandes, N.; Varela, J.; Silva, J.; Simões, M. (2020). Nannochloropsis oceanica Cultivation in Pilot-Scale Raceway Ponds—From Design to Cultivation Applied sciences, 10(5), 1725; <https://doi.org/10.3390/app10051725>.
- [17] Mangelson, K. A. & Watters, G. Z. (1972). The treatment efficiency of waste stabilization ponds. *Journal of the Sanitary Engineering Division, American Society of Civil Engineering*, 98, 407–425. <https://doi.org/10.1061/JSEDAI.0001401>.
- [18] Prussi, M., Buffi, M., Casini, D., Chiaramonti, D., Martelli, F., Carnevale, M., Tredici, M. R., & Rodolfi, L. (2014). Experimental and numerical investigations of mixing in raceway ponds for algae cultivation. *Biomass and Bioenergy*, 67, 390–400. <https://doi.org/10.1016/j.biombioe.2014.05.024>.
- [19] Ranganathan, P., Amal, J. C., Savithri, S., & Haridas, A. (2017). Experimental and modeling of Arthrospira platensis cultivation in open raceway ponds. *Bioresource Technology*, 242, 197–205. <https://doi.org/10.1016/j.biortech.2017.03.150>
- [20] Sompech, K., Chisti, Y., & Srinophakun, T. (2012). Design of raceway ponds for producing microalgae. *Biofuels*, 3, 387–397.
- [21] Liffman, K., Paterson, D. A., Liovic, P., & Bandopadhyay, P. (2012). Comparing the energy efficiency of different high rate algal raceway pond designs using computational fluid dynamics. *Chemical Engineering Research and Design*, 91, 221–226. <https://doi.org/10.1016/j.cherd.2012.08.007>.
- [22] Blanckaert, K., & De Vriend, H. (2004). Secondary flow in sharp open-channel bends. *Journal of Fluid Mechanics*, 498, 353–380. <https://doi.org/10.1017/S0022112003006979>.
- [23] Bonakdari, H., Baghalian, S., Nazari, F., & Fazli, M. (2011). Numerical analysis and prediction of the velocity field in curved open channels using artificial neural networks and genetic algorithms. *Engineering Applications of Computational Fluid Mechanics*, 5, 384–396. <https://doi.org/10.1080/19942060.2011.11015380>.
- [24] Naji-Abhari, M., Ghodsian, M., Vaghefi, M., & Panahpur, N. (2010). Experimental and numerical simulation of flow in a 90° bend. *Flow Measurement and Instrumentation*, 21, 292–298. <https://doi.org/10.1016/j.flowmeasinst.2010.03.002>.
- [25] Shams Ghaffarokhi, G. R., Vrijling, J. K., & Van Gelder, P. H. A. J. M. (2008). Evaluation of superelevation in open channel bends with probabilistic analysis methods. *World Environmental and Water Resources Congress 2008*, Honolulu, Hawaii, 1–14. [https://doi.org/10.1061/40976\(316\)244](https://doi.org/10.1061/40976(316)244).
- [26] Hreiz, R., Sialve, B., Morchain, J., Escudié, R., Steyer, J.-P., & Guiraud, P. (2014). Experimental and numerical investigation of hydrodynamics in raceway reactors used for algaculture. *Chemical Engineering Journal*, 250, 230–239. <https://doi.org/10.1016/j.cej.2014.03.027>.
- [27] Agunwamba, J. C. (1992). Field pond performance and design evaluation using physical models. *Water Research*, 26(10), 1403–1407. [https://doi.org/10.1016/0043-1354\(92\)90133-O](https://doi.org/10.1016/0043-1354(92)90133-O).
- [28] Bernard, O., Lu, L.-D., & Salomon, J. (2020). *Mixing strategies combined with shape design to enhance productivity of a raceway pond*. arXiv:2011.10775. <https://doi.org/10.48550/arXiv.2011.10775>.

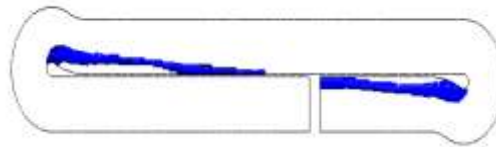
## APPENDIX

Standard



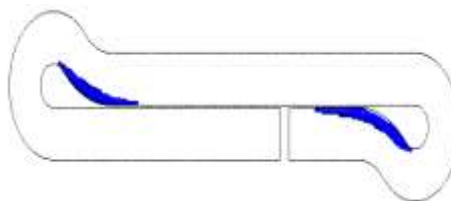
(a)

$R_1=2\text{ m}$

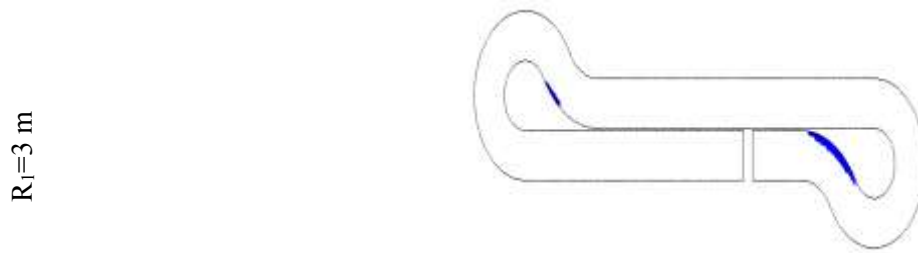


(b)

$R_1=2.5\text{ m}$



(c)



(d)



(e)

Fig. 8: Effect of head radius  $R_1$  on dead zone distribution

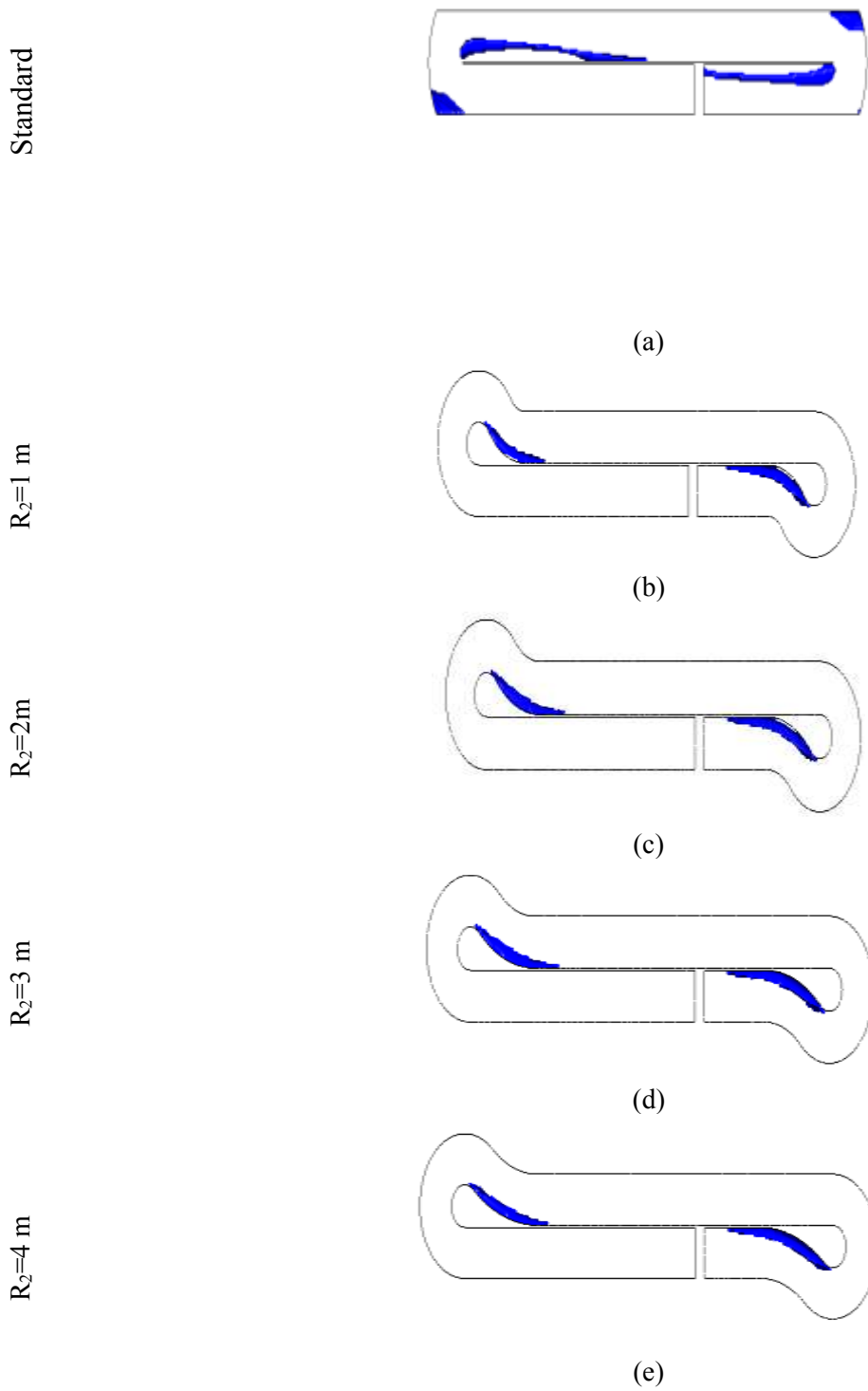


Fig. 9: Effect of medium radius  $R_2$  on dead zones distribution

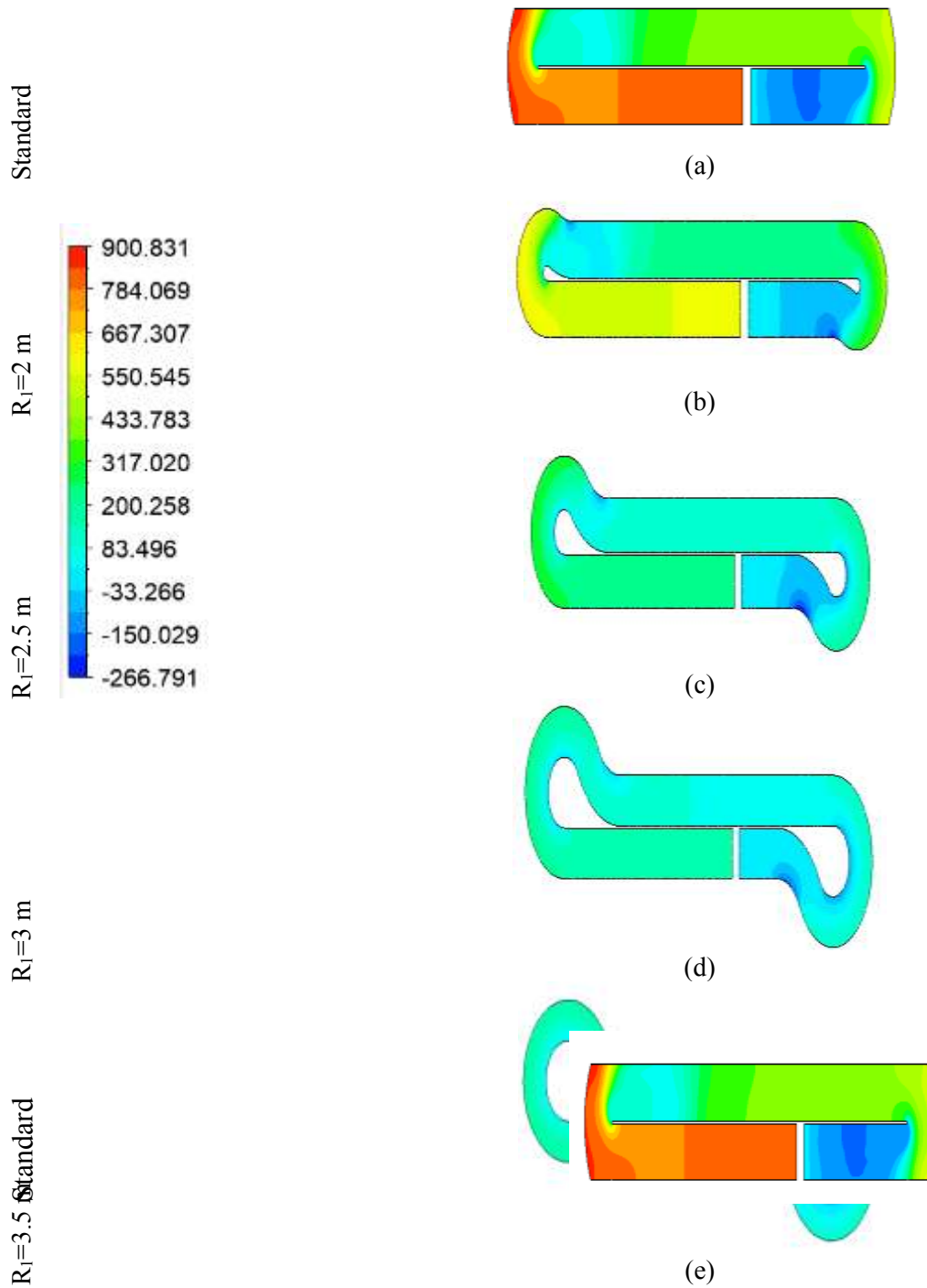


Fig. 10: Static pressure distribution for different  $R_1$



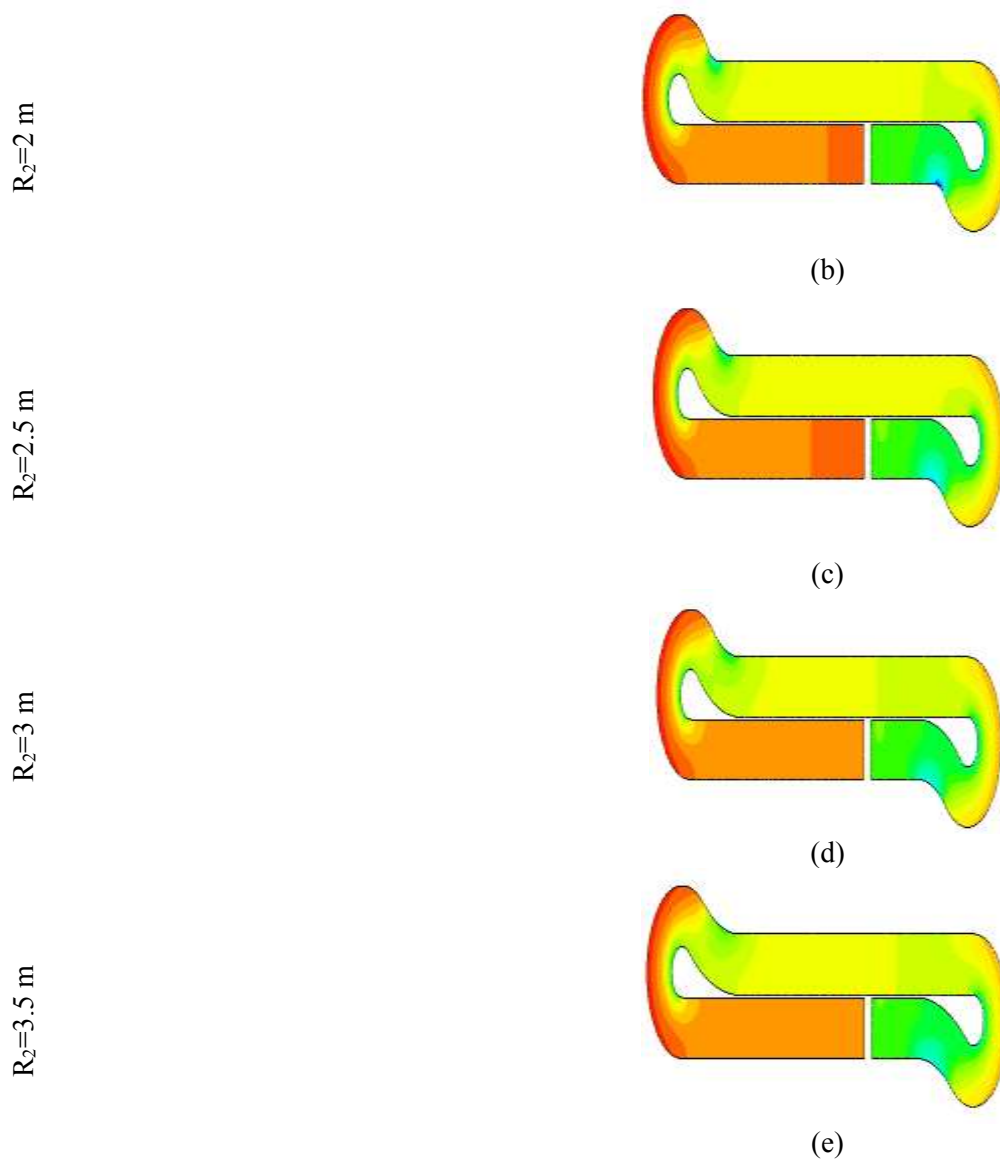


Fig. 11: Static pressure distribution for different  $R_2$

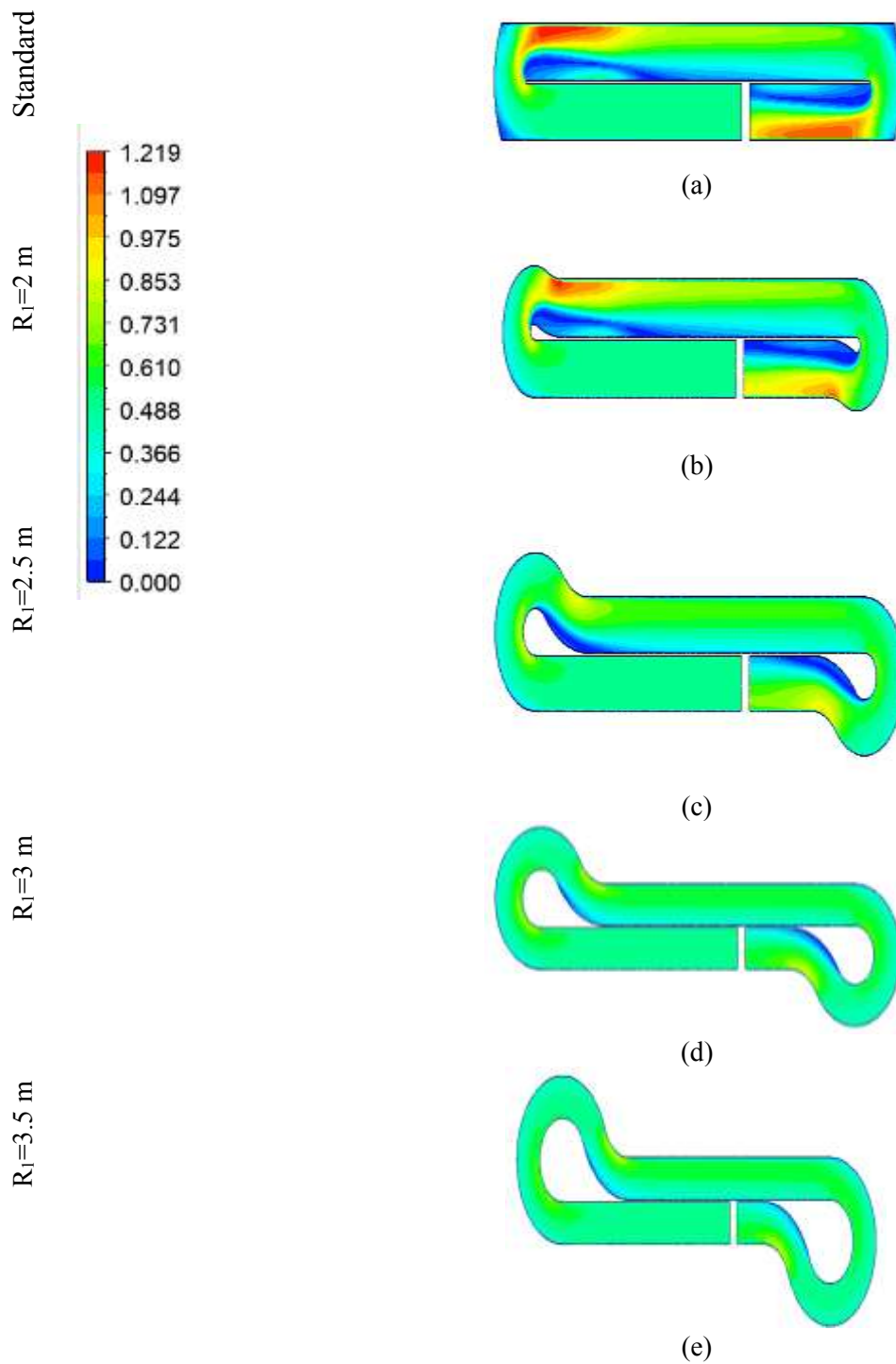


Fig. 12: Distribution of the velocity field with variation in  $R_1$

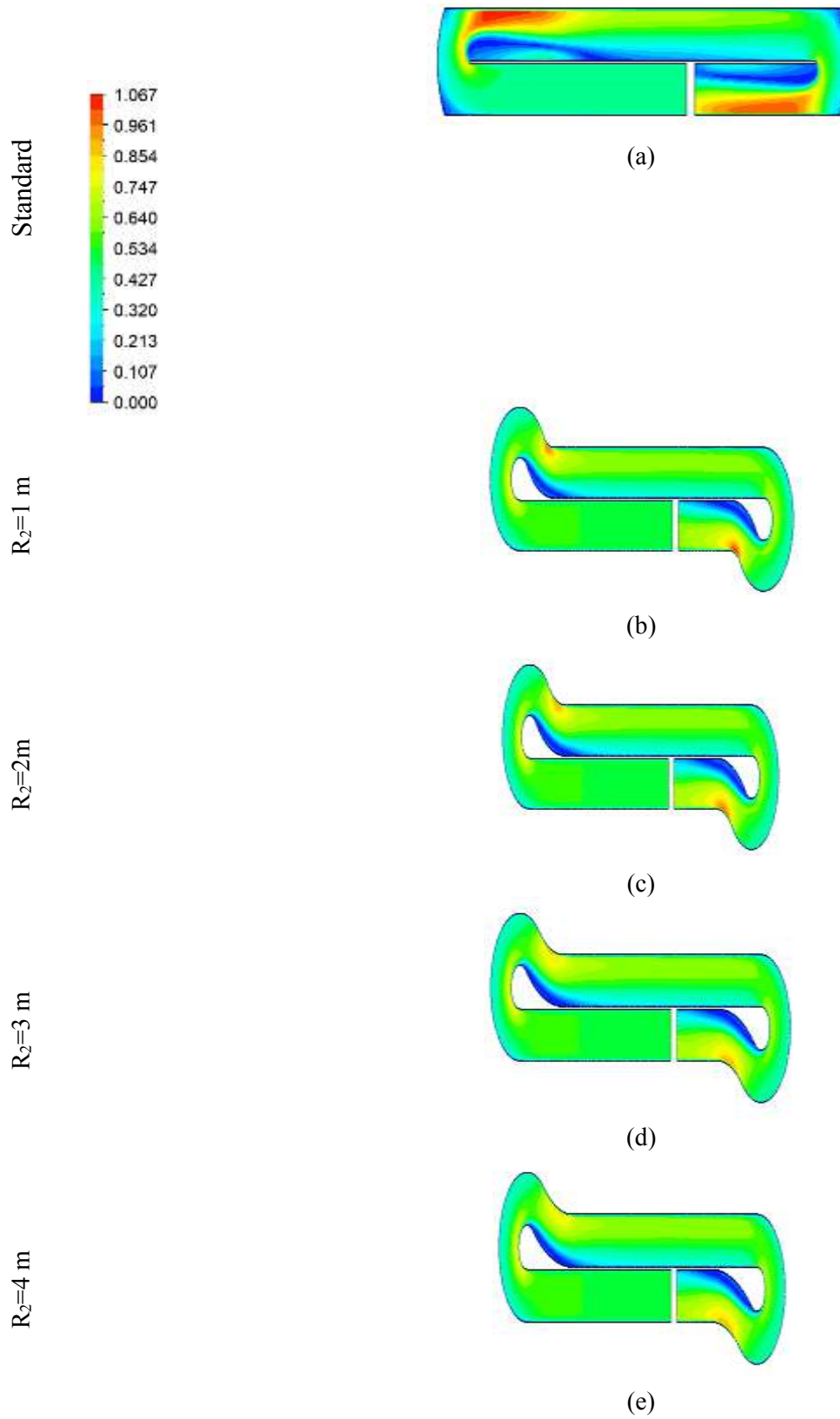


Fig. 13: Distribution of the velocity field with variation in  $R_2$

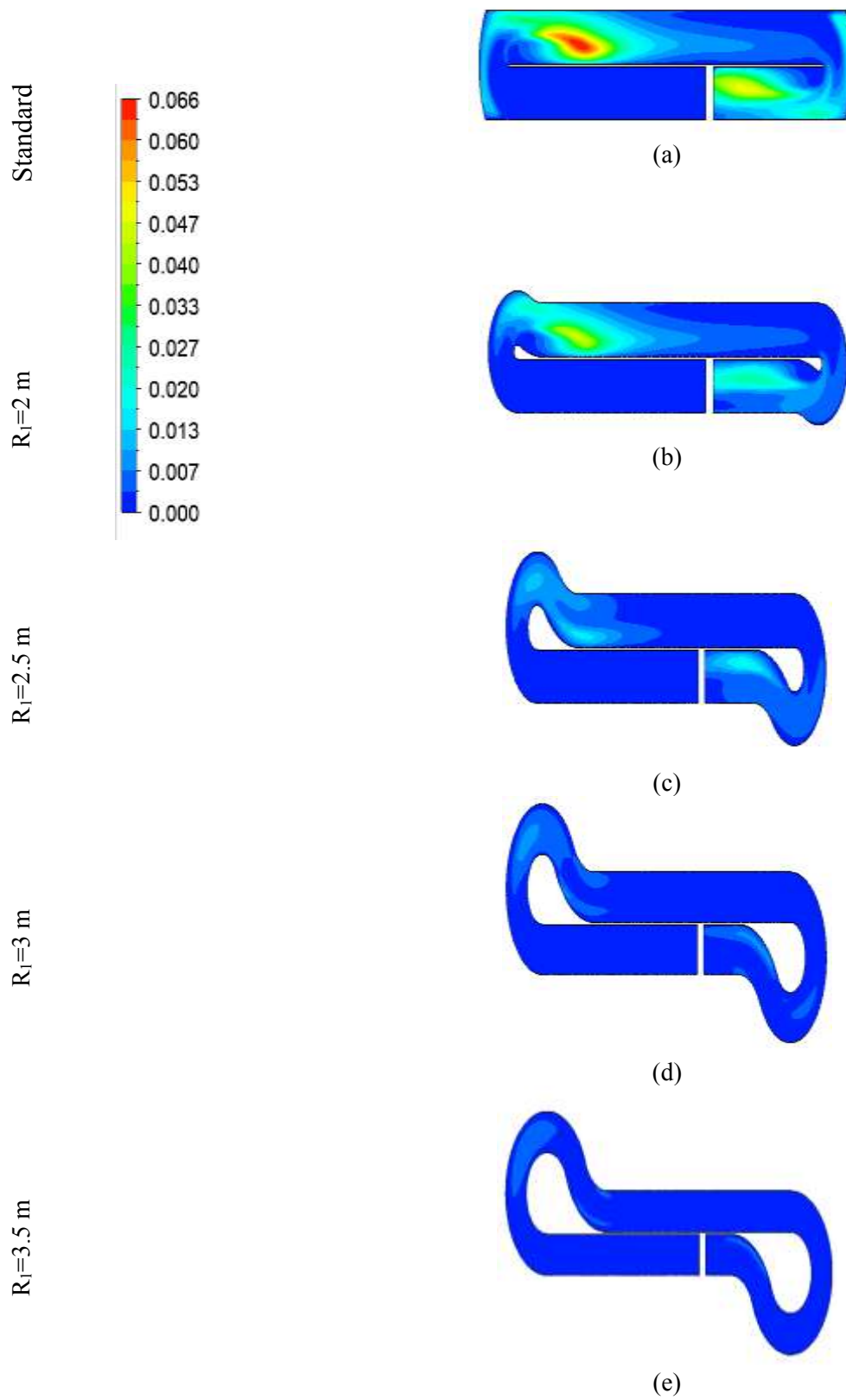


Fig. 14: Turbulent kinetic energy distribution for different  $R_1$

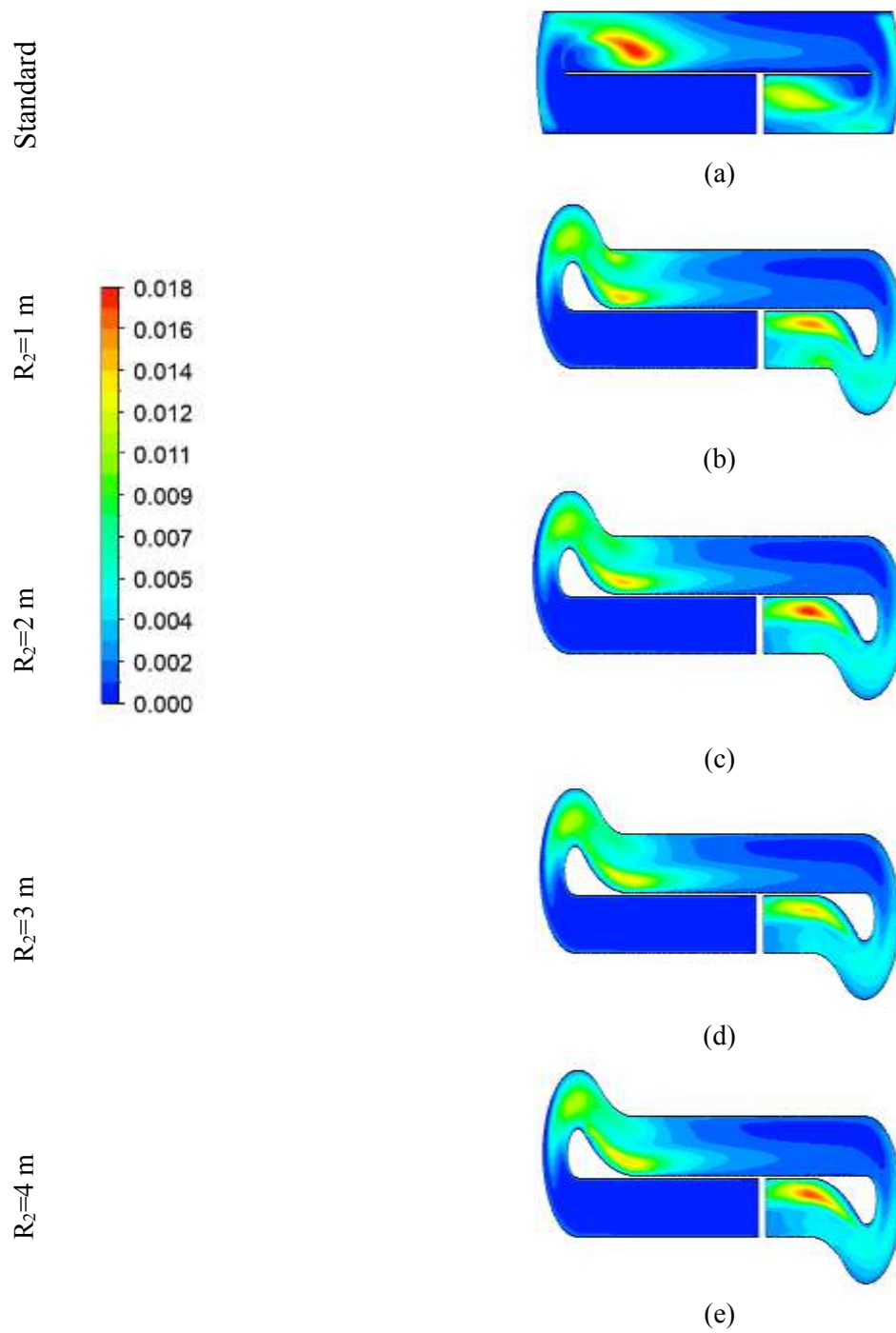


Fig. 15: Turbulent kinetic energy distribution for different  $R_2$



### **Contribution of Individual Authors to the Creation of a Scientific Article (Ghostwriting Policy)**

- Oussama Ghannem: Conceptualized the research, designed the study, and wrote the initial draft of the manuscript, Conducted the experiments, collected data.
- Haythem Nasraoui: contributed to the analysis of results.
- Zied Driss: Provided critical revisions, contributed to the interpretation of data, and helped finalize the manuscript.

### **Sources of Funding for Research Presented in a Scientific Article or Scientific Article Itself**

The authors would like to thank the Laboratory of Electro Mechanic Systems (LASEM) members for the financial assistance

### **Conflict of Interest**

There are no conflicts of interest related to this study. All authors have disclosed any financial or personal relationships that could potentially influence the research.

### **Creative Commons Attribution License 4.0 (Attribution 4.0 International, CC BY 4.0)**

This article is published under the terms of the Creative Commons Attribution License 4.0

[https://creativecommons.org/licenses/by/4.0/deed.en\\_US](https://creativecommons.org/licenses/by/4.0/deed.en_US)